Neutron activation on NILE for quantitative chemical analysis – First results and outlook

Cristina Macia-Castello,[1] Jennifer Huidobro,[2] Daniel Blanco-Lopez,[1] Mattia Gaboardi,[1,3] *Carlo Cazzaniga,[4] Nahid Bhuiyan,[4] Jorge S. Dolado,[1,5] Gorka Arana,[2] Juan Manuel Madariaga,[2] and Felix Fernandez-Alonso[1,5,6]*

[1]Materials Physics Center, CSIC-UPV/EHU, Paseo de Manuel Lardizabal 5, 20018 Donostia - San Sebastian, Spain.
[2]Department of Analytical Chemistry, University of the Basque Country UPV/EHU, Barrio Sarriena s/n, E-48940 Leioa, Biscay, Spain
[3]Chemistry Department, University of Pavia & C.S.G.I., 27100 Pavia, Italy.
[4]ISIS Facility, UKRI-STFC, Rutherford Appleton Laboratory, Didcot OX11 0QX, UK.
[5]Donostia International Physics Center (DIPC), Paseo de Manuel Lardizabal 4, 20018 Donostia - San Sebastian, Spain.
[6]IKERBASQUE, Basque Foundation for Science, Plaza Euskadi 5, 48009 Bilbao, Spain.

Abstract. The recently commissioned NILE facility at the ISIS Pulsed Neutron & Muon Source has been employed to perform neutron activation analysis with 14 MeV neutrons from its D-T source. In this first study of its kind on NILE, we have placed an intentional focus on the use of these new experimental capabilities for the study of cementitious materials. Following neutron irradiation, the resulting gamma-ray spectra enable us to assess the current capabilities of NILE for non-destructive and quantitative elemental analysis of specimens of direct industrial relevance, and demonstrate adequate sensitivity levels to both major and trace components, some of which are not accessible with other analytical techniques. The dependence of the spectroscopic data on source-to-sample distance also shows order-of-magnitude gains associated with the ability to implement neutron irradiation within a few mm from the source. All in all, the experimental results presented herein evince the suitability and yet-to-tapped potential of NILE to implement neutron-activation analysis with typical irradiation times well under one hour.

1 Introduction

Recent advances in Compact Neutron Sources (CNSs) have motivated a more detailed assessment of their capabilities relative to established technologies for neutron production and utilization. To this end, this contribution reports our initial efforts to explore the untapped potential of the recently commissioned Neutron Irradiation Laboratory for Electronics (NILE) facility at the ISIS Pulsed Neutron & Muon Source, United Kingdom. NILE produces neutrons either by Deuterium-Tritium (D-T, 14 MeV) or Deuterium-Deuterium (D-D, 2.5 MeV) fusion reactions, using two different sources operating independently at the same

facility [1]. Both neutron sources are commercially available devices designed and manufactured by Adelphi Tech Inc. [2]. As such, they share the same working principle based on the generation of a plasma gas using a microwave-driven Electron-Cyclotron Resonance (ECR) source to ionize deuterium (D-D source), or a mix of deuterium and tritium (D-T source). The ions generated in the plasma are accelerated towards a metallic target using a high-voltage electric field, where they are implanted in the form of a metal hydride. The remaining ions in the plasma strike the previously implanted ones in the target leading to fusion events that release monoenergetic neutrons of 14 or 2.5 MeV for the D-T and D-D sources, respectively. The resulting neutron yield is 10^9 s^{-1} for the D-D source, with the target located at the center of a cylindrical chamber. The minimum source-to-sample distance in this case is 70 mm. The output of the D-T source is one order-of-magnitude higher, that is, 10^{10} s^{-1}. As shown in Fig. 1, the D-T target is located at the nose of the front-end of the assembly, and this geometry allows for a minimum source-to-sample distance of 8 mm when the sample is in direct contact with the exit window of the source. The available neutron energy, nominal neutron yield, and source-to-sample distance are all important parameters for a given application.

With a view on applications of CNSs in both science and industry, this work has placed an intentional focus on the study of construction materials. The NILE D-T source was used to implement Neutron Activation Analysis (NAA), using as a natural starting point a NIST standard of Ordinary Portland Cement (OPC). This exercise enabled us to assess both the longitudinal profile of the neutronic response and elemental composition. NAA is a non-destructive and highly sensitive means to quantify elemental composition, relying on the interaction of neutrons with the nuclei in the sample under investigation via the formation of radioactive isotopes and their subsequent activity decay through the emission of gamma-rays. The resulting gamma-ray spectrum constitutes a rich and unique source of information for the analytical chemist and the cement producer alike, in the form of well-defined features with characteristic energies determined by the respective isotope and associated spectral intensities directly linked to absolute elemental abundance.

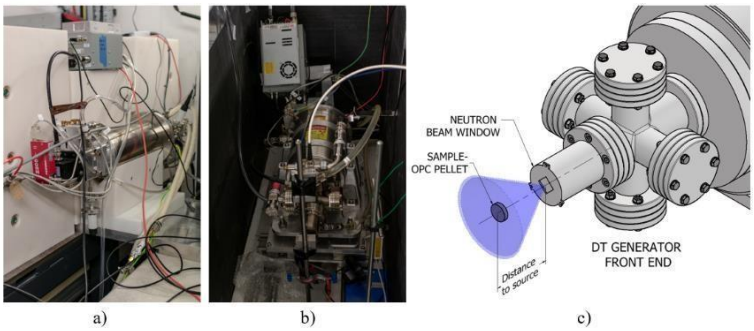

Figure 1. NILE facility in its present incarnation: a,b) photographs of the D-D and D-T sources, respectively; c) sample irradiation geometry of the D-T source. For further details, see the main text.

These results constitute our first feasibility study on NILE and, as such, a necessary starting point for the further optimization of experimental parameters in the pursuit of a more widespread use of these state-of-the-art CNSs, including their use as replacement of isotopic neutron sources, as well as in their concurrent use with other neutron techniques.

2 Methods

A Standard Reference Material of OPC (SRM 634*a* from NIST) was obtained in powder form from the Cement and Concrete Reference Laboratory (CCRL, USA). The certified elemental analysis was performed at NIST [3], combining X-ray fluorescence (XRF) and proficiency test results from CCRL. On a gravimetric basis, the quantitative values of SRM 634*a* can be split between main (>0.1%) and minor (<0.1%) elemental constituents. The main elements include Ca, Si, Al, Fe, S, Mg, K, Ti and P, whereas the minor elements comprise Na, Sr, Mn, Zn or Cr. For this work, five pellets were prepared using a hydraulic press. Applying a pressure of 3 tons to these SRM powders resulted in 1.3-1.7 g cylindrical specimens of 5 mm thickness and 13 mm diameter. These sample dimensions are to be compared with a much-longer neutron mean free path of 84±6 mm, calculated using the above-quoted molar fractions and neutron cross sections at 14 MeV from the EXFOR database [4,5]. All pellets were irradiated for 30-40 minutes using the NILE D-T source at different distances from the target, to establish both elemental composition and the distance dependence of the resulting signal. After irradiation, all samples were transferred to a High Purity Germanium (HPGe) detector setup located in close proximity to NILE. This detector is a coaxial system of the F-profile series from ORTEC, with an energy resolution (FWHM) of 1.95 keV at 1.33 MeV and a nominal relative efficiency of 40%. Energy and efficiency calibrations were performed with a series of gamma-ray laboratory sources supplied by Eckert & Ziegler, including ^{241}Am, ^{137}Cs, ^{133}Ba, ^{54}Mn, and ^{60}Co. These sources are encapsulated within plastic coins and positioned at a standard distance of 5 cm away from the HPGe crystal. The efficiency is then determined from the ratio of the energy-integrated count rate to the gamma-ray emission rate from the source. Subsequently, models of the HPGe detector have been developed utilizing the MCNP6 [6] and GEANT4 [7] Monte Carlo radiation transport codes. The efficiency simulation for a point-like source is then benchmarked against empirical measurements and used for mass determination.

The neutron activation of a stable isotope present in the sample produces radioisotopes that decay via the emission of gamma radiation at well-defined energies [8]. Gamma-spectra were collected at 2-min intervals in the first 10 minutes to detect short-lived products (*e.g.*, ^{28}Al), followed by a long series of 30-min measurements over several hours, to increase signal levels associated with long-lived isotopes. The mass or concentration of a specific element in the sample can be then obtained from the net counts of the gamma line of interest. The amount (in grams) of a specific element was quantified via the use of the following expression [9,10]:

$$m[g] = \frac{I_c}{R\ (1-e^{-\lambda t_i})\ e^{-\lambda t_w}\ (1-e^{-\lambda t_m})\ N_A\ \theta\ I_\gamma} \cdot \frac{\lambda}{M} \qquad (1)$$

Where I_c is the net count of the gamma line (corrected by its full-energy-peak efficiency); N_A is Avogadro´s number; M is the molar mass of the element; $\lambda = ln(2)/t_{1/2}$ is the decay constant of the radioisotope observed in the gamma-ray spectrum and associated with a half-life $t_{1/2}$; t_i is the irradiation time; t_w is the waiting time (*i.e.*, the time elapsed from the end of the irradiation period and the start of the first measurement of the gamma-ray spectrum); and t_m corresponds to the measurement time of the gamma-ray spectrum. These times were determined with absolute errors down to one second. I_γ in Eq. (1) corresponds to the intensity of the gamma-

ray of interest and θ is the abundance of the isotope considered. Finally, *R* (in units of s^{-1}) is the activation rate per nucleus of a given isotope, defined as the product between the cross section of the relevant nuclear reaction and the neutron flux ϕ, namely,

$$R = \sigma(14\,MeV)\ \phi \qquad (2)$$

Flux characterization was performed with an iron foil during this particular experimental campaign, following the procedures described in Ref. [11]. A more extensive characterization was performed prior to these, as reported in Ref. [1]. A fission chamber detector was used to monitor the flux and stability of the beam during all measurements.

3 Results and discussion

Figure 2 shows the gamma-ray spectrum obtained for an OPC pellet of mass 1.57 g placed at 38 mm from the neutron source. Elemental speciation was performed by assigning each peak to the corresponding radioisotope. Elements like Ca, Fe, Si, or Al can be easily accessed and were observed and quantified with ease. Furthermore, traces of Sr and K can also be detected and quantified. The fraction (*wt*.%) of a given element calculated after peak fitting and integration are also reported in Table 1, and compared to the values provided by NIST. Neutron cross-section data were taken from Ref. [5] using the ENDF/B-VIII.0 library. To evaluate uncertainties, we considered several contributions like detector efficiency, flux, waiting time, and peak intensities. As a combination of these contributions, we estimated a relative uncertainty of *ca.* 15%, similar to what is reported in NAA studies [10].

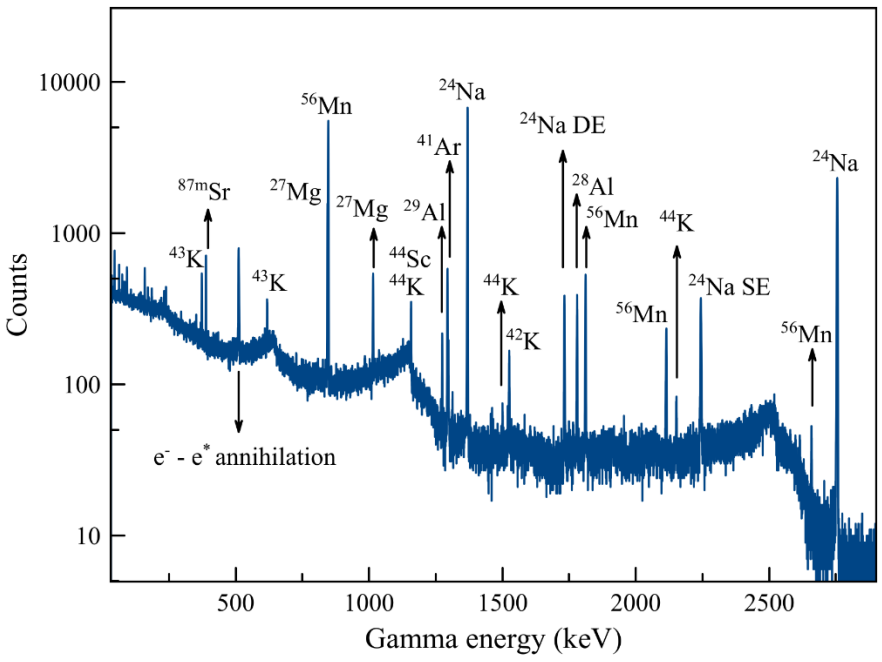

Figure 2. Gamma-ray spectrum and radionuclide assignments of an OPC pellet of mass 1.57 g, recorded for 33 minutes after irradiation. The pellet was irradiated at 38 mm from the neutron source. Note the logarithmic scale of the ordinate axis.

Table 1 reports several elements present in the OPC specimen described in the previous Section, as well as the relevant nuclear reactions for major (>0.1%) and minor constituents. We note that O was not detected and, therefore, not quantified as the corresponding radionuclides decay too rapidly to be detected with the present experimental setup. The possibility of implementing gamma-ray measurements *in-situ* is being assessed as a potential future development on NILE. We also note that ^{44}K and ^{44}Sc share some lines in the gamma-ray spectrum, yet in our case this emission arises from ^{44}K. ^{44}Sc can be produced from the ^{45}Sc(n,2n)^{44}Sc nuclear reaction, yet it is also a trace element that is not seen in the XRF analysis performed at NIST. Furthermore, for an irradiation time of just over half four, the built-up factor is more favourable for ^{44}K than for ^{44}Sc due to its shorter half-life.

Table 1. Columns, from left to right: element; relevant nuclear reactions at 14 MeV; half-lives ($t_{1/2}$) of the produced radionuclides; gamma-ray energies (E); peak intensites (3% uncertainty); neutron capture cross sections (σ); and NIST and NAA values. For further details on the NIST values, see Section 2. Only peaks with more than 100 counts have been included in this Table. The asterisks in the gamma-ray energies denote the most intense features, used in the calculations of elemental concentrations – *cf.* Eq (1). The nuclear data have been obtained from Refs. [5,8,12].

Element	Nuclear reaction	$t_{1/2}$	E (keV)	Intensity (counts)	σ (mb)	*wt%* (NIST)	*wt%* (NAA)
Si	^{28}Si(n,p)^{28}Al	2.24 min	1778.99	325±10	279.41	9.55±0.07	9.39±1.41
Al	^{27}Al(n,α)^{24}Na	14.99 h	1368.625* 2754.03	9576±287	122.51	2.67±0.02	2.95±0.44
Fe	^{56}Fe(n,p)^{56}Mn	2.58 h	846.77* 1810.72 2113.09	7304±219 1900±57 450±14	114.05	2.34±0.03	2.46±0.37
Ca	^{44}Ca(n,p)^{44}K	22.13 min	1157.02	266±8	40.15	46.5±0.3	38.8±5.5
K	^{41}K(n,p)^{41}Ar	109.6 min	1293.64	873±26	48.16	0.292±0.004	0.8±0.1
Sr	^{88}Sr(n,2n)^{87}Sr	2.81 h	388.51	470±14	877.48	0.062±0.005	0.019±0.003

As shown in Table 1, the characteristic gamma-ray peaks corresponding to typical elements present in OPC have been identified with success, demonstrating the suitability of NILE for this type of study. The NAA values for elements exceeding a concentration of 1% are closer to the NIST figures than those with concentrations below 1%. The origin of these discrepancies for the latter are being explored via additional measurements with other standards.

As an important parameter to characterize the capabilities of the current D-T source on NILE, Fig. 3 shows measurements at progressively increasing distances from the target – 8, 28, 38, 48 and 58 mm from the neutron source. The masses of the irradiated pellets was 1.5, 1.38, 1.57, 1.54 and 1.68 g, respectively. The average neutron flux (cm^{-2} s^{-1}) over an irradiation period t_i can be written as

$$\phi = \frac{N}{t_i \, 4\pi \, d^2} \tag{3}$$

where d is the distance between the sample and the source and N is the total number of neutrons emitted by the source over this period. The neutron yield is of *ca.* 10^9 s^{-1} at an operating voltage of 110 kV. The actual flux depends on distance and scales as d^{-2}. At a position of 3.8 cm from the source, the flux is, therefore, *ca.* 10^7 cm^{-2} s^{-1}. This figure can vary quite significantly depending on the various operational parameters of the neutron generation such as voltage, gas pressure or microwave power.

Within a given irradiation period, the neutron flux can undergo fluctuations as a function of time. These are primarily related to the stability of the generator, caused by factors like variations in the pressure and temperature of the plasma. Typically, these variations are small. In this analysis, we have approximated the flux to be constant, using as a value the average neutron flux during the measurement. In the future, we will attempt a more complex analysis, where variations as a function of time are taken into account. As shown in Ref. [1], this approximation is sufficient to attain uncertainties below 10%, which are sufficient for our purposes.

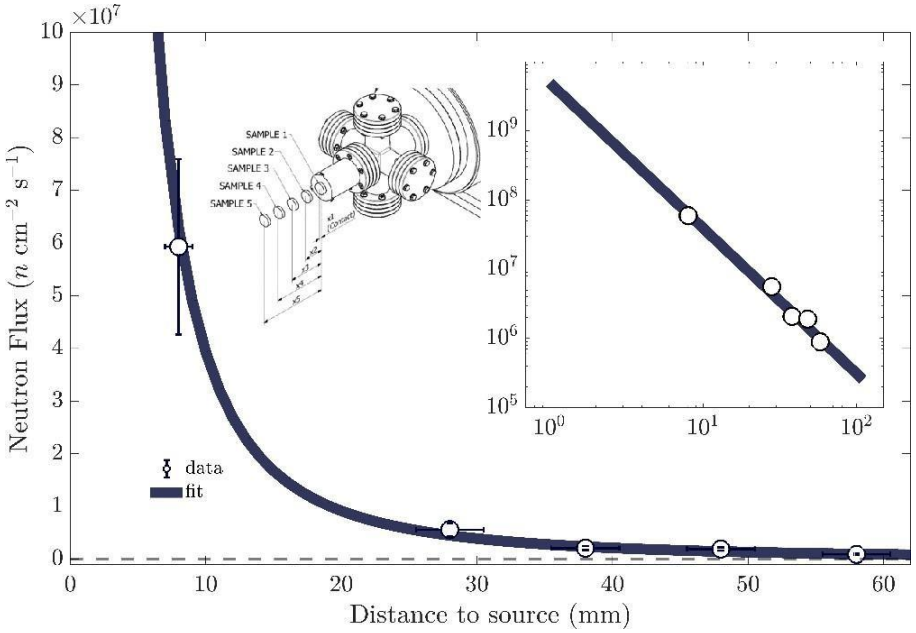

Figure 3: Response of the NILE D-T source as a function of source-to-sample distance. The insets show a schematic diagram of the experimental setup (left) as well as the experimental data displayed in the main figure in a *log-log* representation (right inset). The latter plot highlights the expected d^{-2} dependence of these data.

As shown in Fig. 3, distance is a critical and key parameter to optimise experimental conditions for this type of CNS. Relative to the closest source-to-sample distance of 8 mm,

there is an order of magnitude loss in signal by the time the sample is a mere 30 mm away. The data were fitted to a power-law of the form $y = \alpha\ d^{-\beta}$, giving an exponent $\beta = 2.08 \pm 0.17$, and confirming the expected dependence with distance. These results indicate that this type of D-T source easily outperforms other available sources as well as an equivalent D-D source, both in terms of total neutron yield as well as in terms of a favourable geometry that enables irradiation in close proximity to the target. In addition, most of the nuclear reactions considered herein have energy thresholds above the neutron energy of a D-D source, 2.5 MeV.

4 Conclusions and outlook

The current D-T source of the recently commissioned NILE facility was employed for the first time to study the elemental composition of cementitious materials via NAA. Major elemental constituents like Ca, Fe, Si, Al were detected and quantified with relative ease and in relatively short times, with an estimated uncertainty of 15% for the current experimental setup. Moreover, trace elements were also identified and quantified. Elements like O could not be detected, and this shortcoming motivates further developments for *in-situ* irradiation and measurement, in order to detect short-lived species. On the other hand, the possibility of performing NAA measurements near the source can lead to order-of-magnitude enhancements in performance relative to other 14-MeV neutron-production facilities available elsewhere. Further down the road, we envisage implementing prompt-gamma neutron activation analysis on NILE, paving the way for the quantification of a wider range of chemical elements.

5 Acknowledgments

We thank the UK Science & Technology Facilities Council for access to the NILE facility at the ISIS Pulsed & Muon Source – doi.org/10.5286/ISIS.E.RB2320039. We also acknowledge the continued support received from the IKUR Strategy under the collaboration agreement between Ikerbasque Foundation and the Materials Physics Center on behalf of the Department of Education of the Basque Government.

6 References

1. C. Cazzaniga, *et al.* (2023) 'Characterization measurements of compact neutron generators of the new Nile Facility,' *IEEE Transactions on Nuclear Science*, 70(8), pp. 1616–1624. doi:10.1109/tns.2023.3293797
2. adelphitech.com/ (Accessed 22 March 2024).
3. *Standard Reference Material 634a*, tsapps.nist.gov/srmext/certificates/634a.pdf (Accessed 22 March 2024).
4. N. Otuka, *et al.* (2014) 'Towards a more complete and accurate experimental nuclear reaction data library (EXFOR): International collaboration between nuclear reaction data centres (NRDC),' *Nuclear Data Sheets*, 120, pp. 272–276. doi:10.1016/j.nds.2014.07.065.
5. *Nuclear Data Center at KAERI – Table of Nuclides.* Available at: atom.kaeri.re.kr/nuchart/ (Accessed 22 March 2024)
6. A. Sood (2009) 'Recent developments for MCNP6,' Report No. LA-UR-09-1056.
7. G. Cosmo (2024) *Geant4-11.2.0, Geant4*. Available at: geant4.web.cern.ch/download/11.2.0.html (Accessed 22 March 2024).

8. *Livechart – Table of Nuclides, Nuclear Structure and Decay Data*. Available at: www-nds.iaea.org/relnsd/vcharthtml/VChartHTML.html (Accessed 22 March 2024).
9. K. S. Krane, and D. Halliday, *Introductory Nuclear Physics*, 3rd Edition (Wiley, 1987).
10. C. Cazzaniga *et al.* (2021) 'Neutron activation analysis of archeological artifacts using the ISIS pulsed neutron source,' *AIP Advances*, 11(7). doi:10.1063/5.0043935.
11. D. Chiesa *et al.* (2018) 'Measurement of the neutron flux at spallation sources using multi-foil activation,' *Nuclear Instruments and Methods in Physics Research Section A: Accelerators, Spectrometers, Detectors and Associated Equipment*, 902, pp. 14–24. doi:10.1016/j.nima.2018.06.016
12. S.Y.F. Chu, L.P. Ekström, R.B. Firestone, *WWW Table of Radioactive Isotopes, Database Version 1999-02-28.* Available at nucleardata.nuclear.lu.se/toi/ (Accessed 22 March 2024).